Incipient Separation of a Supersonic Turbulent Boundary Layer at High Reynolds Numbers

Gary S. Settles,* Seymour M. Bogdonoff,† and Irwin E. Vas‡
Princeton University, Princeton, N. J.

Two-dimensional compression corner and axisymmetric flare geometries were used in this study of shock wave interaction with a compressible turbulent boundary layer. The study was carried out at a Mach number of 2.9 and over a Reynolds number range of $10^5 < \mathrm{Re}\delta_0 < 10^7$ (Re_X up to 10^9). Detailed surface pressure, schlieren, and oil-flow data were obtained for several corner angles. A major finding of this study is that incipient separation is a gradual rather than an abrupt phenomenon. Incipient separation corner angles were found to be within a band of about 16°-18° and essentially independent of Reynolds number over the range studied.

Nomenclature

C_f	= skin friction coefficient
M	= Mach number
p	= pressure, psia
Re	= unit Reynolds number, $\rho_\infty u_\infty / \mu_\infty$
T	= temperature, °R
u	= velocity, fps
x	= distance along model surface from corner, in.
X	= distance along model centerline from tip, also distance along tunnel centerline from nozzle throat, in.
Y	= distance normal to model surface, in.
$\Delta X/\delta_0$	= upstream influence parameter (see Fig. 7)
$\Delta\mathrm{Sep}/\delta_0$	= distance from separation line to compression corner normalized by δ_0
α	= ramp or flare angle, deg.
δ	= boundary-layer thickness, in.
δ^*	= boundary-layer displacement thickness, in.
θ	= boundary-layer momentum thickness, in.
μ	= viscosity coefficient
ρ	= density

Subscripts

T	= stagnation conditions
∞	= freestream conditions
0	= undisturbed incoming flow condition near corner
c	= corner condition
i	= condition of incipient separation

I. Introduction

INCIPIENT turbulent boundary-layer separation is an area of fluid mechanics which has been of major interest for many years, because a knowledge of it is important in the design of high-speed aircraft, turbomachinery, etc. Lacking a sound theory for turbulent boundary-layer behavior in the presence of a strong adverse pressure gradient, investigators have adopted an experimental approach to the problem. Much was learned about separation in general from the early experiments of Bogdonoff et al.[1] and Chapman et al.,[2] and about incipient separation in particular from Kuehn's work.[3] Some questions were also raised by these studies, notably concerning how the conditions necessary for incipient separation might vary with increasing Reynolds number. The need of a basis for extrapolating Kuehn's results up to flight Reynolds numbers led to more recent studies in which flight Re_X levels were achieved in the wind tunnel. The results of these studies, however, were in disagreement concerning the level and Reynolds number trend of the compression corner angle necessary for incipient separation at about Mach 3. While Kuehn had found that α_i decreased as $\mathrm{Re}\delta_0$ increased, Roshko and Thomke[4,5] and Law[6] reported a reversal of this trend at higher Reynolds numbers, and Settles and Bogdonoff,[7] and Rose et al.[8] found no effect of Reynolds number change. Further, recent work by Spaid and Frishett[9] raised questions about previously established incipient separation conditions at lower Reynolds numbers. While part of this disagreement may be traced to the different experimental methods used to indicate incipient separation, our knowledge and understanding of this phenomenon nevertheless leave much to be desired.

The present work is an attempt to clarify the subject of incipient turbulent boundary-layer separation at moderate to high Reynolds numbers. To do this, a unique experimental facility capable of reaching a given Reynolds number two or three different ways and of operating over a broad Re_X range has been employed. The experiments described here have been designed with an eye toward obtaining highly detailed data on a scale much smaller than one boundary-layer thickness. Also, a unified approach is used in drawing conclusions from the data, wherein a number of different indicators of incipient

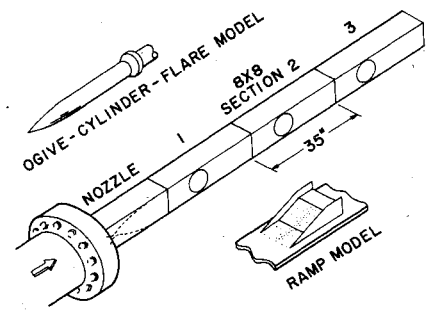

Fig. 1 Diagram of 8 × 8 supersonic wind tunnel with test models.

Presented as Paper 75-7 at the AIAA 13th Aerospace Sciences Meeting, Pasadena, Calif., January 20-22, 1975; submitted January 20, 1975; revision received June 3, 1975. This research was supported by the Office of Aerospace Research, Aeronautical Research Laboratories, Wright-Patterson, Air Force Base, under Contracts F33615-70-C-1244 and F33615-73-C-4156.

Index categories: Boundary Layers and Convective Heat Transfer—Turbulent, Supersonic and Hypersonic Flow.

*Graduate Research Assistant, Department of Aerospace and Mechanical Sciences, Gas Dynamics Laboratory; now Research Scientist at Princeton Combustion Laboratories/Flow Research, Inc., Princeton, N.J. Member AIAA.

†Professor and Chairman, Department of Aerospace and Mechanical Sciences, Gas Dynamics Laboratory. Fellow AIAA.

‡Senior Research Engineer and Lecturer, Department of Aerospace and Mechanical Sciences, Gas Dynamics Laboratory. Associate Fellow AIAA.

separation are applied and the results compared. The first phase of this study[7] reported preliminary results concerning incipient separation. The present phase updates and expands this work considerably, confirming the earlier conclusions. The third phase, concerning the details of separated turbulent flows, is now awaiting publication.

Because of space limitations, many details of the experiments cannot be included here. The reader is encouraged to consult the other references[7,10-12] for a more complete discussion of this material.

II. Description of Experiment

A. Wind Tunnel

This experimental study was performed in the Princeton University high Reynolds number $8\times8-$in. supersonic air-tunnel.[13] The 8×8 is a blowdown tunnel which provides test times ranging from 30 sec to several minutes at stagnation pressures of 50-500 psia, a nominal Mach number of 2.9, and about ambient stagnation temperature. Test models in the 8×8 have near adiabatic wall conditions.

The tunnel proper consists of a nozzle followed by three constant area sections, as shown in Fig. 1. The sections are interchangeable, so that an experimental geometry may be mounted on the tunnel wall at any of three different distances downstream of the nozzle throat. Combined with the stagnation pressure capability of the wind tunnel, this leads to two specific advantages over the usual fixed-model-type tunnel: a broad Reynolds number range, and the ability to crisscross Reynolds numbers, obtaining a given Re_X through large X and small $p_{t\infty}$ or small X and large $p_{t\infty}$.

The Reynolds number range of the present set of experiments carried out on the tunnel wall extends from $Re_X=0.4\times10^8-9\times10^8$ ($Re_{\delta_0}=0.5\times10^6-7.6\times10^6$). This capability covers the Reynolds number range normally experienced by large high-speed aircraft in flight. Further, experiments carried out on a sting-mounted centerbody in tunnel section 1 developed Re_{δ_0}'s between 0.14×10^6 and 0.6×10^6, overlapping the tunnel wall capability and ex-

B. Models and Instrumentation

1. Ramp Compression Corner

A ramp compression corner geometry was chosen to provide the adverse pressure gradient to which the tunnel wall boundary layer would be subjected. Solid brass ramps with corner angles of 10°, 14°, 16°, 18°, and 20° were fitted into the tunnel wall, as diagramed in Fig. 1.

The compression ramps themselves were 6 in. wide, allowing an inch on either side of the model to bypass the tunnel sidewall boundary layers. Side fences were installed to isolate the corner flow further and to prevent spillage where a separated region was present.

Each model included some 47 static pressure taps of 0.032-in. diameter. The taps were distributed upstream of the compression corner and along the ramp surface, but were spaced as closely as $0.03\delta_0$ in the vicinity of the corner itself.

2. Ogive-Cylinder Flare

A second experimental geometry, the ogive-cylinder-flare model, also sketched in Fig. 1, was mounted on a sting support and carefully aligned along the tunnel section 1 centerline. This geometry was chosen to investigate incipient separation at moderate Reynolds numbers and to provide a check on the ramp data in the range of Reynolds number overlap of the two geometries. The model has a 6-in.-long ogival nose joined smoothly to a 2-in. diameter cylindrical section. Axisymmetric flares were mounted 14 in. back from the model tip, where the boundary layer was found to be less than 15% of the body radius in thickness. Surface pressure data and schlieren photos were obtained from the model over a range of test conditions. A full description of this model and its calibration is available.[7,10]

C. Boundary Layers

During the initial calibration of the 8×8-in. tunnel a complete set of surveys was obtained to determine wall boundary-layer mean velocity profiles. Complete details of this calibration are available.[11] The turbulent boundary layer on the ogive-cylinder model was similarly investigated.[7,10]

Table 1 Summary of ramp compression corner boundary-layer data

SECTION	M_∞	Pt_∞	SYMBOL	δ_0, in.	δ^*_0, in.	θ_0, in.	$Re_{\delta_0}\times10^{-6}$	$Re/in.\times10^{-6}$	c_{f_0}
1	2.95	60	○	0.520	0.131	0.023	0.52	1.00	0.00140
		100	◒	0.490	0.129	0.023	0.78	1.60	0.00129
		200	◐	0.463			1.46	3.20	
		300	◒	0.440	0.104	0.018	2.07	4.75	0.00110
		400	◐	0.429			2.68	6.30	
		500	●	0.416	0.098	0.017	3.25	7.90	0.00102
2	2.89	60	□	0.870	0.242	0.043	0.87	1.00	0.00126
		100	▬	0.830	0.243	0.042	1.33	1.60	0.00115
		200	▮	0.781			2.46	3.20	
		300	▬	0.740	0.195	0.035	3.48	4.75	0.00099
		400	▮	0.718			4.49	6.30	
		500	■	0.698	0.183	0.032	5.44	7.90	0.00092
3	2.84	60	△	1.185	0.343	0.065	1.19	1.00	0.00117
		100	▲	1.140	0.317	0.060	1.82	1.60	0.00110
		200	▲	1.080			3.47	3.20	
		300	▲	1.042	0.233	0.042	4.90	4.75	0.00096
		400	▲	1.010			6.31	6.30	
		500	▲	0.980	0.240	0.04?	7.64	7.90	0.00090

Table 2 Summary of flare compression corner boundary-layer data

TAP NO.	M_∞	Pt_∞	SYMBOL	δ_0, in.	δ^*_0, in.	θ_0, in.	$Re_{\delta_0}\times10^{-6}$	$Re/in.\times10^{-6}$	c_{f_0}
20	2.91	60	○	0.1515	0.051	0.0091	0.137	0.90	0.0016?
		100	◒	0.1470	0.049	0.0088	0.218	1.48	0.00149
		200	◐	0.1405	0.044	0.0079	0.412	2.93	0.0013?
		300	◒	0.1345	0.041	0.0074	0.592	4.40	0.00129

Tables 1 and 2 summarize the parameters of the two test boundary layers. A symbol has been assigned to each test condition to avoid confusion. For both model and tunnel wall boundary layers, favorable comparison with the Law of the Wall and Wake showed them to be fully turbulent and in an equilibrium condition.

III. Results

A. Static Pressure Distributions

1. Ramp

Static pressure measurements on each of the five ramp models were carried out at six stagnation pressures (60, 100, 200, 300, 400, and 500 psia) in each of the three tunnel sections. The 90 individual pressure distributions thus obtained in the basic data set are arranged in 18 subsets, one at each available test Reynolds number. One such set of data is shown in Fig. 2. In this figure, dimensional pressures are normalized by the upstream wall static pressure p_0, and distances measured from the compression corner are normalized by the incoming δ_0. Final pressure ratios predicted by inviscid theory are shown to the right of the data for each corner angle. The pressure tap diameter normalized by δ_0 amounts to about half the size of the symbols used. Data points shown at $x/\delta_0 = 0$ correspond to pressures actually measured in the corner itself.

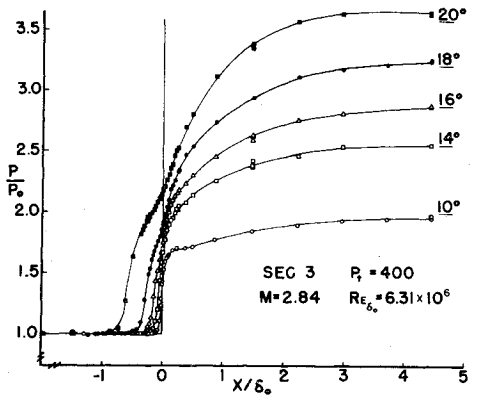

Fig. 2 Example plot of static pressure distributions on ramp models.

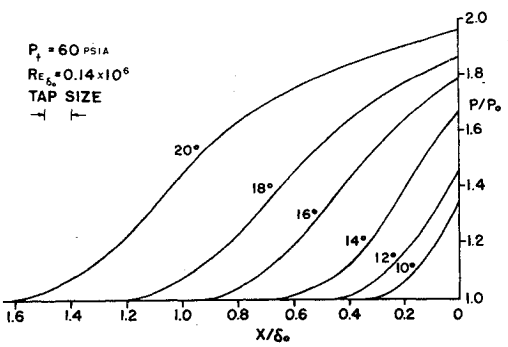

Fig. 3 Example plot of static pressure distributions ahead of flare models.

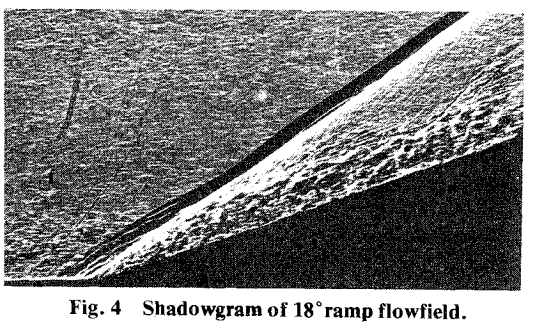

Fig. 4 Shadowgram of 18° ramp flowfield.

2. Flare

Preliminary measurements of the pressure-rise curves ahead of several flares have been reported.[7] These measurements were made by monitoring the pressure at a surface tap while the flare was moved up to and over the tap. The measurements were later found to contain errors due to slippage in the flare drive mechanism. This condition has been corrected, and an example of the revised data is shown in Fig. 3 for flare angles of 10°-20° in 2° increments.

B. Shadow and Schlieren Photographs

Flow visualization photographs by means of either direct shadow or schlieren optics were obtained for all ramp and flare test conditions. One such photograph of flow from left to right over the 18° ramp model is shown in Fig. 4. Accumulated photographic evidence indicates that the size of such interactions fluctuates on a scale much smaller than one boundary-layer thickness.

Of particular interest in this photograph is the dual character of the shock wave, a straight "main" shock well off the model surface and a "separation shock" or "induced shock" at a somewhat shallower angle near the compession corner. Such a shock shape is similar to that of an attached inviscid supersonic flow over a double-angle ramp. The separated region in the corner is not visible here because of its small vertical extent.

C. Surface-Flow Patterns

For a majority of the ramp test conditions, surface-flow patterns were obtained by a technique involving the use of a mixture of kerosene and graphite particles. A small quantity of this mixture was distributed well upstream of the ramp before a test. Upon startup, the mixture streamed down the tunnel wall and coated the ramp model. Tiny graphite particles collected in a liquid line upstream of the corner. The kerosene quickly evaporated during the test, leaving a very thin graphite pattern resembling pencil marks on the model after shutdown. The graphite patterns were preserved by lifting them off the model with transparent tape and pressing them down on white paper.

An example kerosene-graphite surface flow pattern on the 14° ramp model is shown in Fig. 5. Note that the separation line is straight and parallel to the corner, as was approximately the case with most of the other surface-flow patterns obtained, and that reattachment is much less visible than separation in this photo. The graphite accumulation line is referred to with confidence as the separation line, because the evaporation of the kerosene during a test eliminates any liquid ridge, which might otherwise have been displaced from the true separation location.

Separation distances ahead of the compression corner were easily measured from the surface-flow patterns. These separation distances are normalized by the proper δ_0's and plotted vs ramp angle in Fig. 6 for nine test conditions. The curves seem to asymptote toward zero separation at zero corner angle. In fact, tiny separated regions on the order of one millimeter in extent were observed even at $\alpha = 10°$, the lowest corner angle investigated in this study.

IV. Discussion of Results

A. Upstream Influence Parameter

Consider a typical compression corner static pressure distribution, as diagrammed in Fig. 7. Regardless of whether or not the flow is separated, data shown here and elsewhere[9,14] indicate that the surface pressure always begins to rise before the actual corner is reached, that is, there is always some upstream influence. If one draws a line tangent to the

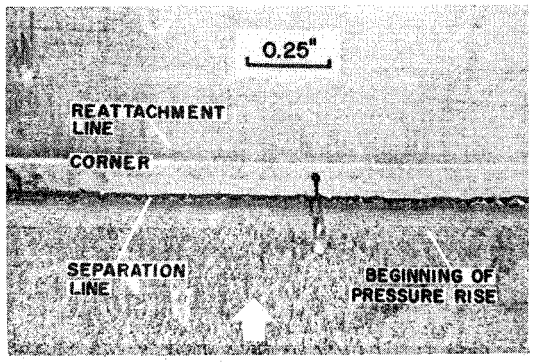

Fig. 5 Example of kerosene-graphite surface-flow pattern.

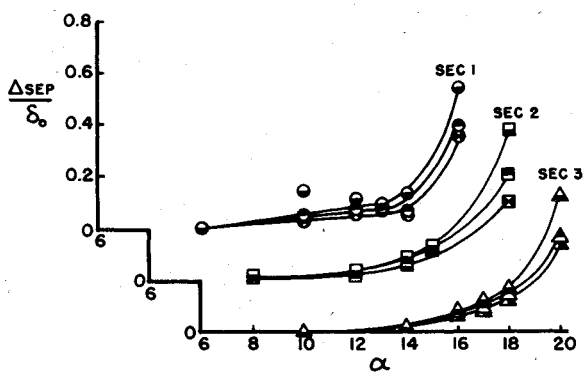

Fig. 6 Normalized separation distances vs ramp corner angle.

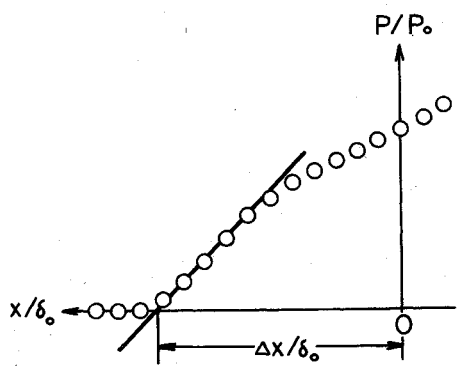

Fig. 7 Diagram of a typical compression corner static pressure distribution, defining $\Delta x/\delta_0$, the upstream influence parameter.

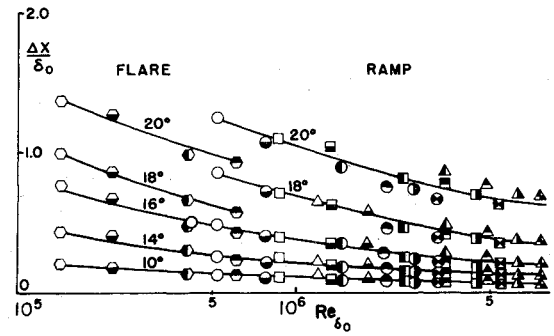

Fig. 8 Variation of ramp and flare upstream influence parameter with Reynolds number.

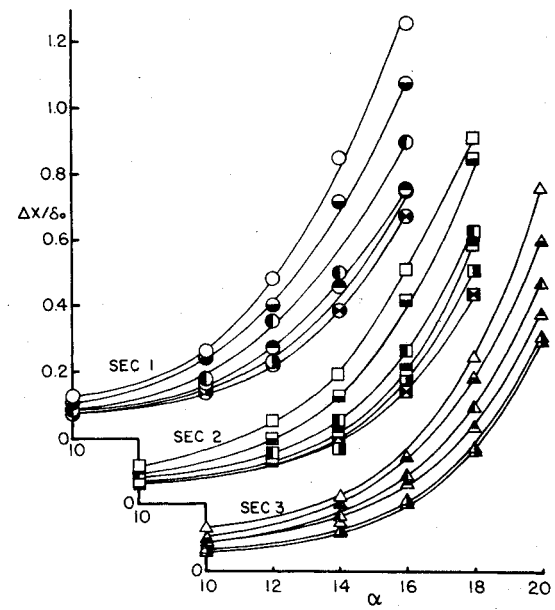

Fig. 9 Plot of upstream influence parameter vs ramp corner angle.

maximum slope of the surface pressure curve upstream of the corner and extrapolates this line to the X/δ_0 axis, one can define an upstream influence parameter, $\Delta X/\delta_0$, as shown in the diagram. This parameter is easier to obtain and more consistent than the actual beginning of the pressure rise.

Some parameter describing upstream influence length, such as $\Delta X/\delta_0$, is very important in characterizing shock-boundary-layer interactions. Through its use, much can be learned about the size and behavior of such interactions. In the present study, values of $\Delta X/\delta_0$ have been extracted from the ramp and flare data at each test condition. The variation of this upstream influence data with Reynolds number is shown graphically in Fig. 8.

From the figure, a consistent trend of decreasing upstream influence with increasing Reynolds number is apparent. At supersonic Mach number and moderate to high Reynolds numbers, all other known investigations[4-6,15,16] have confirmed this trend. The Reynolds number overlap of data points from the three tunnel sections is clearly shown in Fig. 8, as is the overlap in ramp and flare Reynolds numbers. Ramp upstream influence points from the three tunnel sections collapse accurately onto single curves for each of the lower corner angles. A slight divergence of ramp data from the different sections, or "unit Reynolds number effect," appears in the 18° and 20° ramp data. This divergence is not serious enough to obscure the overall trend of the data at these ramp angles. Significantly, for $\alpha = 10°$, 14°, and 16°, both ramp and flare data collapse onto the same curves. This fact has important implications about the two-dimensionality of the ramp data, which will be discussed in Sec. IV B.

The data in Fig. 8 are cross-plotted as X/δ_0 vs α in Fig. 9, with Reynolds number as a parameter. This crossplot shows that upstream influence is a very regular function of corner angle and that families of such curves result from Reynolds number variation. A similar set of curves is found for the flare data. In Fig. 9, upstream influence appears to rise almost exponentially with corner angle. In fact, a simple Reynolds number-dependent shifting in the horizontal direction succeeds reasonably well in collapsing all the ramp upstream influence data onto a single exponential curve, as shown in Fig. 10.

The regularity of the upstream influence curves, when considered alongside the separation distance curves of Fig. 6, leads to an important conclusion. Figure 6 showed that the separation distance, as determined from surface-flow patterns, grows from nonexistent or tiny proportions to significant proportions over the 10°-20° ramp angle range considered here. This fact is not obvious, however, from the upstream influence curves of Fig. 9 and 10. In the latter curves, no clue is given to indicate the presence of a developing separated flow in the corner region, other than the

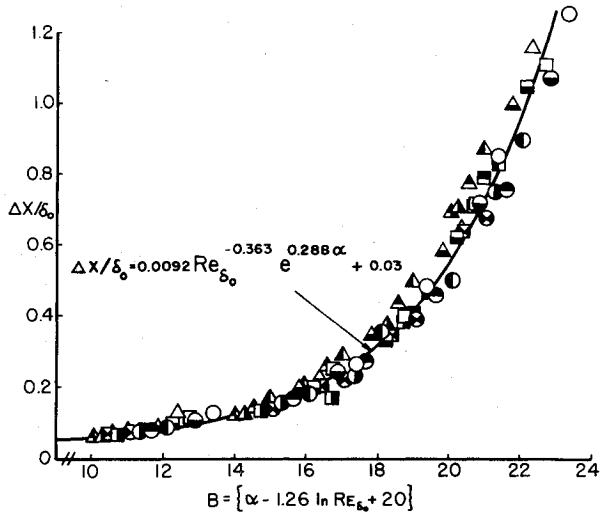

Fig. 10 Ramp upstream influence data of Fig. 9 collapsed upon a single exponential curve.

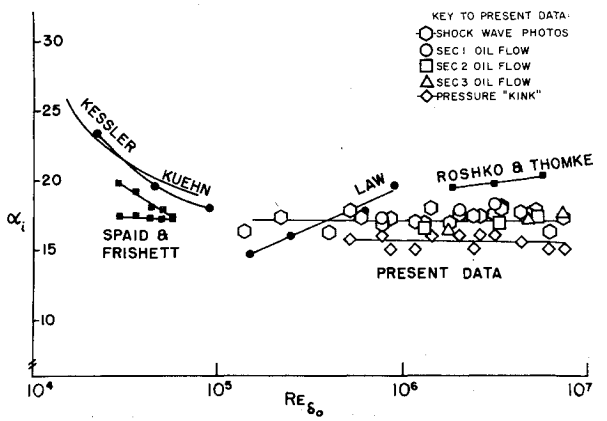

Fig. 11 Summary of Reynolds number effect on compression corner angle for incipient separation at about Mach 2.9.

mere fact that upstream influence is increasing with corner angle. There are no sharp breaks in the curves. The important conclusion is that incipient separation, insofar as it affects gross properties of the interaction like upstream influence, is a very gradual rather than an abrupt phenomenon.

B. Two-Dimensionality

Shock boundary-layer interaction studies in rectangular channels are always subject to serious questions about end effects and other possible departures from two-dimensionality. Recent investigations by Reda and Murphy[17,18] and Green[19] have shown that, at least for incident-shock interactions, such departures may seriously confuse the meaning of experimental data.

In view of this, a hard look at two-dimensionality is vital in any study of the present type. Constant transverse pressures and straight separation lines were found in the present study, but are necessary but not sufficient conditions for two-dimensionality. A much better check on two-dimensionality is the comparison between ramp and flare data at the same Reynolds number. The axisymmetric flare interaction is inherently free of end effects. Also, for attached corner flows, the scale of the interaction is small compared to the body radius, so the flow may be assumed locally two-dimensional. The incoming mean profiles for ramp and flare boundary layers at the same $Re_{\delta 0}$ are very similar. Under these circumstances, the previously discussed favorable comparison of low-angle ramp and flare upstream influence data indicates that, since the flare data are two-dimensional, the ramp data are also two-dimensional. This agreement supports the two-dimensionality of the present attached and incipient ramp data. The surface-flow patterns and transverse-row pressure data support the two-dimensionality of all the ramp data in this study, including those cases with sizeable separation for which the ramp-flare comparison no longer applies. In such cases, the flare interaction is a mixed 2-D and conical flow, and thus is no longer comparable to the ramp interaction.

C. Incipient Separation

Incipient separation in a shock boundary-layer interaction has traditionally been defined as the condition in which the shear stress becomes vanishingly small at some point on the wall, while reamining positive elsewhere. Under such a condition, increasing the adverse pressure gradient slightly causes the appearance of a "separation bubble" containing reverse flow. Kuehn[3] first pointed out that this definition is clouded, at least in the case of a compression corner geometry, due to the apparent fact that some tiny separated region is always present, even for very low corner angles. Based on present findings, this is indeed the case. One is forced, then, to discard the preceding definition for practical purposes, in favor of some indicator that the ever-present separation bubble is reaching significant proportions, and is beginning to divert the interaction from what are normally considered "attached" conditions.

Kuehn recognized this fact also, and chose the first appearance of a "kink" or triple inflection point in the compression corner surface pressure distribution as his revised condition for incipient separation. In other investigations a number of different techniques have been applied either to sense the presence of separation itself, or to discover under what conditions separation becomes important. Techniques of the former type and their users are: 1) Surface oil-flow patterns.[1,2,6,8,9,15,17-19] 2) Direct measurements of skin friction or heat transfer in the corner region.[20] 3) A surface pitot traverse in the corner region.[1] 4) Orifice-dam readings of the surface-flow direction.[4]

On the other hand, criteria used to determine at what corner angle separation becomes significant are: 1) Upstream influence length and/or separation distance plotted vs corner angle and extrapolated to zero.[5,6,9,15,18,21] 2) A break or inflection in curves of pressure near the corner vs corner angle.[5,6,9,21] 3) The first appearance of a "separation" or "induced" shock wave.[7,9,14] 4) The first appearance of a "kink" in the surface pressure distribution.[3,9,20,22]

As mentioned in Sec.I, the application of these criteria in several experimental studies has resulted in disagreement over the level of α_i, the incipient separation corner angle, and its trend with Reynolds number variation at a fixed Mach number. Since different experimenters used different criteria in determining α_i, the fact that the results disagree is not too surprising. The following discussion examines each criterion as it applies to the present data and its comparison with that of other investigators.

1. Separation Lengths From Surface-Flow Data

The ramp separation length curves of Fig. 6 all begin to turn more sharply upward in the range of 16° to 18° corner angles. This is a strong indication that separation is becoming significant within this corner angle range. Since the separation distance curves are without sharp breaks, it is difficult to be more specific than this in determining values of α_i. One arbitrary method is to pick values of α_i where the separation curves cross the line $\Delta_{sep}/\delta_0 = 0.1$. These values must be assigned a reasonably large band because, although the separation data themselves are precise, the onset of significant separation is gradual and difficult to pin down. Similar reasoning applies to the upstream influence curves of Fig. 9.

2. Appearance of the Separation Shock Wave

For low angle corner flows no separation or induced shock is observed. The first appearance of a separation shock as α increases is another indicator of the onset of significant separation. By plotting shock angles vs corner angle, incipient separation angles may be determined. Once again, the separation shock tends to emerge gradually, so it is misleading to talk in terms of exact values for α_i. The four flare α_i points and 18 ramp points evaluated in this manner fell almost entirely between 16° and 18°. Over the approximately two-decade $Re_{\delta 0}$ range of this study, no systematic variation of these α_i values with Reynolds number was found.

3. Kink in Static Pressure Distributions

Kuehn's method of choosing α_i at the first appearance of a kink in the static pressure distribution was applied to the ramp data. Since these data are highly detailed in the vicinity of the compression corner, the kink criterion is particularly sensitive. Incipient separation angles obtained by this criterion fell generally between 15° and 16°. Once again, no net variation with Reynolds number was observed.

4. Variation of Corner Pressure with Angle

Crossplots of the detailed surface pressure data obtained in this study show a nearly linear rise of compression corner pressure as corner angle is varied from 10° through 20°. There are no breaks or other features in the data to suggest incipient separation. However, pressures near the *reattachment* point do tend to level off for corner angles greater than 20°, as determined from recent tests of 24° and 28° ramp models. This seems to indicate that the corner pressure criterion gives erroneously high values when used to indicate incipient separation, and is only effective *after* the separation bubble has become sizable. Thus, the discrepancy between present α_i results and the higher values found by Roshko and Thomke[4] becomes easier to understand: Their results were obtained by using the corner pressure and orifice-dam criteria, both of which are relatively insensitive to small regions of separation.

5. Summary of Incipient Separation

Figure 11 shows the present incipient separation data in comparison with that of others who worked near Mach 2.9, on the traditional plot of α_i vs $Re_{\delta 0}$. The band of the present data lies largely between 15° and 18°, depending on the technique used to determine incipient separation, and is constant with respect to Reynolds number. This result conflicts with the increasing trends reported by Roshko and Thomke and Law over the same Reynolds number range. The reasons behind this conflict bear considerable discussion.

One of the firm conclusions to be drawn from this study is that the incipient separation phenomenon is basically a smooth and gradual transition between "attached" and "separated" flows rather than an abrupt change. Once this is understood, the reason for the wide band of the present data becomes clear. If one considers only the three α_i points obtained by an arbitrary means from surface-flow measurements in tunnel section 1, then an increasing trend similar to that observed by Roshko and Thomke is found. By the same token, decreasing trends may be found within the scatter of the present α_i points. However, an overall look at the present data leaves no doubt that incipient separation is found to be without significant Reynolds number dependence. Since incipient separation angles are inherently imprecise, consideration of only three or four data points may cause misleading conclusions to be drawn concerning the effect of Reynolds number. Further, varying Reynolds number only through a change in $p_{t\infty}$, with a fixed length of turbulent run, may not reveal the true trend of incipient separation conditions. (Compare, for example, the section, 1, 2, or 3 surface-flow determined α_i points of Fig. 11 with the overall trend of all the data.)

A second reason for the disagreement of the present data with Law and with Roshko and Thomke has to do with the fact that, as Reynolds number increases, decreasing upstream influence or separation size has often been assumed to indicate rising values of α_i. That assumption is questioned in the present investigation. While Figs. 8 and 9 clearly show that upstream influence decreases as $Re_{\delta 0}$, is raised, and Fig. 6 indicates the same conclusion for separation distance, the incipient separation results are, nonetheless, without Reynolds number dependence. This raises serious questions about the advisability of extrapolating separation or upstream influence lengths to zero to determine α_i, a procedure which has been used by a number of investigators.[6,9,15,17,18,21,22] The regular progression with Reynolds number change of curves like those in Fig. 9 will always *seem* to indicate that α_i is increasing with $Re_{\delta 0}$ when extrapolation from the higher angles in employed. Present evidence shows this to be a false indication. Further, the fact that such curves are smooth exponentials makes linear extrapolation very difficult to justify.

A reexamination of previously published Mach 3 incipient separation data in the light of these findings is of interest. The sharp breaks in upstream influence curves in the authors' preliminary work are clearly in error, though the incipient separation results of that study are supported here. Reexamination of Law's data is hindered by the fact that he worked with large corner angles and extrapolated downwards toward incipient separation. Nevertheless, application of the "kink" criterion to Law's pressure distributions yields incipient separation levels roughly 2°-5° greater than those he reported, with a much smaller upward trend as $Re_{\delta 0}$ increases. The same criterion applied to the pressure distributions of Roshko and Thomke appears roughly to confirm the α_i values they reported. Its application was inaccurate, however, due to the approximately $\frac{1}{4}\delta_0$ spacing of their pressure taps. As for the data of Spaid and Frishett, their kink and p_c vs α results (those shown in Fig. 11) are not in serious enough disagreement to fall outside a reasonable incipient separation band. Their oil-flow results support the present conclusion that small separated regions exist in a compression corner, even at low, "attached flow" corner angles. Kuehn's careful measurements,[3] as well as those of Kessler et al.[22] are, unfortunately, compromised by the fact that tripped boundary layers were employed. Thus, the state of affairs for incipient separation at $Re_{\delta 0}$'s between 10^4 and 10^5 is still in question. At moderate and high Reynolds numbers the present study shows an α_i level of about 15°-18° with no Reynolds number dependence. Disagreement with other investigators in this range appears to be as much a question of interpretation as of actual measurements.

V. Conclusions

The present investigation of supersonic turbulent boundary layer interactions with axisymmetric flare and two-dimensional ramp compression corners was carried out at about Mach 2.9 with $Re_{\delta 0}$ varying between 1.4×10^5 and 7.6×10^6 and wall temperatures near adiabatic. The results of this investigation support the following major conclusions: 1) Incipient separation is a gradual rather than an abrupt phenomenon. 2) The corner angle for incipient separation falls within a band of 15°-18°, depending on the criterion used, and is independent of Reynolds number over the range studied.

Also, the following observations have been made:

1) Nominally attached flows at low corner angles have tiny separated regions imbedded within them at the corner location. Thus, the rigid definition is discarded in favor of a more practical one for incipient separation: the corner angle at which separation begins to become significant.

2) As Reynolds number was raised, compression corner upstream influence lengths were found to decrease. This seems to imply an increasing trend of incipient separation angle, but in fact no such trend was found.

3) Two-dimensionality of the ramp compression corner results is shown by a favorable comparison with the axisymmetric flare results at the same Reynolds number.

4) The nature of the incipient separation phenomenon may cause its determination to be misleading if only a few data points are taken, or if only the density factor in the Reynolds number is varied.

5) Detailed measurements show that compression corner upstream influence lengths increase roughly exponentially with corner angle.

6) Extrapolating large upstream influence or separation lengths to zero size or plotting compression corner pressure vs corner angle are not valid ways of finding incipient separation angles.

References

[1]Bogdonoff, S.M., Kepler, C.E., and Sanlorenzo, E., "A Study of Shock Wave Turbulent Boundary-Layer Interaction at Mach 3," PUAED Rept. 222, 1953, Princeton University, Princeton, N.J.

[2]Chapman, D.R., Kuehn, D.M., and Larson, H.K., "Investigation Of Separated Flows in Subsonic and Supersonic Streams with Emphasis on the Effects Of Transition," NACA Rept. 1356, 1958.

[3]Kuehn, D.M., "Experimental Investigation of the Pressure Rise Required for the Incipient Separation of Turbulent Boundary Layers in Two-Dimensional Supersonic Flow," NASA Memo 1-21-59A, 1959.

[4]Roshko, A. and Thomke, G.J., "Incipient Separation of a Turbulent Boundary Layer at High Reynolds Number in Two-Dimensional Supersonic Flow over a Compression Corner," Rept. DAC 59819, 1969, McDonnell Douglas, Huntington Beach, Calif.

[5]Roshko, A. and Thomke, G.J., "Flare-Induced Separation Lengths in Supersonic Turbulent Boundary Layers," *AIAA Journal,* Vol. 13, to be published.

[6]Law, C.H., "Supersonic Turbulent Boundary-Layer Separation," *AIAA Journal,* Vol. 12, June 1974, pp. 794-797.

[7]Settles, G.S. and Bogdonoff, S.M., "Separation of a Supersonic Turbulent Boundary Layer at Moderate to High Reynolds Numbers," AIAA Paper 73-666, Palm Springs, Cal., 1973.

[8]Rose, W. C., Page, R. J., and Childs, M. E., "Incipient Separation Rise for a Mach 3.8 Turbulent Boundary Layer," *AIAA Journal,* Vol. II, May 1973, pp. 761-763.

[9]Spaid, F. W. and Frishett, J. C., "Incipient Separation of a Supersonic Turbulent Boundary Layer, Including Effects of Heat Transfer," *AIAA Journal,* Vol. 10, July 1972, pp. 915-922.

[10]Settles, G.S, Bogdonoff, S.M., and Vas, I.E., "Incipient Separation of a Supersonic Turbulent Boundary Layer , At Moderate To High Reynolds Numbers," AIAA Paper 75-7, Pasadena, Calif., 1975.

[11]Vas, I.E., Settles, G.S., and Bogdonoff, S.M., "The Characteristics of a Supersonic Turbulent Boundary Layer at High Reynolds Numbers," Gas Dynamics Lab., Princeton University, in preparation.

[12]Settles, G.S., "An Experimental Study of Compressible Turbulent Boundary Layer Separation at High Reynolds Numbers," Ph.D. Thesis, Aerospace and Mechanical Sciences Dept., Princeton University, Princeton, N.J., Sept. 1975.

[13]Vas, I.E. and Bogdonoff, S.M., "A Preliminary Report on the Princeton University High Reynolds Number 8×8-In. Supersonic Tunnel," Internal Memo. 39, 1971, AMS Dept. Gas Dynamics Lab. Princeton University, Princeton, N.J.

[14]Drougge, G., "An Experimental Investigation of the Influence of Strong Adverse Pressure Gradients on Turbulent Boundary Layer at Supersonic Speeds, " FFA Rpt. 47, Swedish Aeronautical Establishment, Stockholm, Sweden, 1953.

[15]Appels, C., "Incipient Separation of a Compressible Turbulent Boundary Layer," Von Karman Institute for Fluid Dynamics TN 9, Brussels, Belgium, 1974.

[16]Hammitt, A.G. and Hight, S., "Scale Effects in Turbulent Shock Wave Boundary-Layer Interactions," AFOSR TN 60-82, Sept. 1959, Air Force Office of Scientific Research, Arlington, Va.

[17]Reda, D.C. and Murphy, J.D., "Shock Wave/Turbulent Boundary-Layer Interactions in Rectangular Channels," *AIAA Journal,* Vol. 11, Feb. 1973, pp. 139-140.

[18]Reda, D.C. and Murphy, J.D., "Sidewall Boundary-Layer Influence on Shock Wave/Turbulent Boundary-Layer Interactions," *AIAA Journal,* Oct. 1973, pp. 1367-1368.

[19]Green, J.E., "Reflexion of an Oblique Shock Wave by a Turbulent Boundary Layer," *Journal of Fluid Mechanics,* Vol. 40, Jan. 1970, pp. 81-95.

[20]Holden, M.S., "Shock Wave—Turbulent Boundary-Layer Interaction in Hypersonic Flow," AIAA Paper 72-74, San Diego, Calif., 1972.

[21]Elfstrom, G.M., "Turbulent Separation in Hypersonic Flow," Imperial College, University of London, Aero Rept. 71-16, Sept. 1971.

[22]Kessler, W.C., Reilly, J.F., and Mockapetris, L. J., "Supersonic Turbulent Boundary Layer Interaction with an Expansion Ramp and a Compression Corner," Rept. MDC E0264, Dec. 1970, McDonnell Douglas, Huntington Beach, Calif.